Biol. Chem., Vol. 392, pp. 1097–1111, December 2011 • Copyright © by Walter de Gruyter • Berlin • Boston. DOI 10.1515/BC-2011-200

Dimerization of human 5-lipoxygenase

Ann-Kathrin Häfner[1], Mihaela Cernescu[2], Bettina Hofmann[1], Michael Ermisch[1], Michael Hörnig[1], Julia Metzner[1], Gisbert Schneider[3], Bernhard Brutschy[2] and Dieter Steinhilber[1,*]

[1] Institute of Pharmaceutical Chemistry/ZAFES, University of Frankfurt, Max-von-Laue-Strasse 9, 60438 Frankfurt, Germany

[2] Institute of Physical and Theoretical Chemistry, University of Frankfurt, Max-von-Laue-Strasse 9, 60438 Frankfurt, Germany

[3] ETH Zurich, Department of Chemistry and Applied Biosciences, Institute of Pharmaceutical Sciences, Wolfgang-Pauli-Strasse 10, CH-8093 Zurich, Switzerland

*Corresponding author
e-mail: steinhilber@em.uni-frankfurt.de

Abstract

Human 5-lipoxygenase (5-LO) can form dimers as shown here via native gel electrophoresis, gel filtration chromatography and LILBID (laser induced liquid bead ion desorption) mass spectrometry. After glutathionylation of 5-LO by diamide/glutathione treatment, dimeric 5-LO was no longer detectable and 5-LO almost exclusively exists in the monomeric form which showed full catalytic activity. Incubation of 5-LO with diamide alone led to a disulfide-bridged dimer and to oligomer formation which displays a strongly reduced catalytic activity. The bioinformatic analysis of the 5-LO surface for putative protein-protein interaction domains and molecular modeling of the dimer interface suggests a head to tail orientation of the dimer which also explains the localization of previously reported ATP binding sites. This interface domain was confirmed by the observation that 5-LO dimer formation and inhibition of activity by diamide was largely prevented when four cysteines (C159S, C300S, C416S, C418S) in this domain were mutated to serines.

Keywords: diamide; 5-lipoxygenase; LILBID; leukotrienes; molecular modeling.

Introduction

5-Lipoxygenase (5-LO) is the key enzyme in the formation of leukotrienes (LTs) (Werz, 2002) which play an important role in inflammatory diseases like asthma and atherosclerosis (Dahlén et al., 1980; Funk, 2001). Recently, the 5-LO gene was identified as a regulator of leukemia stem cell proliferation in BCR-ABL-induced chronic myeloid leukemia (CML) (Chen et al., 2009). 5-LO catalyzes a two-step reaction, first the conversion of arachidonic acid (AA) into 5(S)-hydroperoxy-6-trans-8,11,14-cis-eicosatetraenoic acid (5-HPETE), second the conversion of 5-HPETE into the allylic epoxide leukotriene A4 (LTA_4). This unstable epoxide can be further metabolized to the biologically active LTB_4 by LTA_4 hydrolase or to the cysteinyl leukotriene LTC_4 by LTC_4 synthase (Shimizu et al., 1986).

Mammalian 5-LO consists of 672–673 amino acids (Matsumoto et al., 1988). The 5-LO structure published recently (Gilbert et al., 2011) confirms that human 5-LO consists of an N-terminal regulatory C2-like domain (residues 1–114) and a C-terminal catalytic domain (residues 121–673) which is mainly organized in α-helices and contains the non-heme iron in its catalytic center. The C2-like domain is responsible for the association of 5-LO to the nuclear membrane (Chen and Funk, 2001; Kulkarni et al., 2002), for diacylglyceride (Hörnig et al., 2005) and calcium binding (Hammarberg et al., 2000) and for the interaction with coactosin-like protein (Rakonjac et al., 2006).

In the cell, 5-LO activity can be regulated by many factors. An increase in intracellular calcium leads to translocation of the enzyme from the cytosol to the nuclear membrane (Peters-Golden and Brock, 2003), where 5-LO co-localizes with 5-LO-activating protein (FLAP) and cytosolic phospholipase A_2 ($cPLA_2$) (Pouliot et al., 1996). An alternative modulation of 5-LO activity is phosphorylation at distinct serine residues. Phosphorylations at Ser-271 by MAPKAP kinase 2 (Werz et al., 2000) and at Ser-663 by ERK2 (Werz et al., 2002) have a stimulatory effect, whereas phosphorylation at Ser-523 by protein kinase A (PKA) inhibits the activity (Luo et al., 2004). In most reviews, 5-LO is mentioned as a monomeric enzyme (Rouzer and Samuelsson, 1985; Rådmark, 2002), nevertheless, it was previously shown that 5-LO from rat basophilic leukemia cells (RBL-1) forms dimers in the presence of calcium (Parker and Aykent, 1982). Recently, Shang et al. analyzed dimerization and flexibility of rabbit 12/15-LO and human 12-LO by small angle X-ray scattering (SAXS) (Shang et al., 2011). The outcome of their study was that (i) r12/15-LO is mainly monomeric, but dimerizes at higher protein concentrations and with increasing protein flexibility, and (ii) that human 12-LO is stable as a dimer confirming their former studies for 12-LO (Aleem et al., 2008). Moreover, studies of Zhang et al. provided an additional hint for a 5-LO dimer (Zhang et al., 2000). They performed affinity and photoaffinity labeling experiments with 5′-*p*-fluorosulphonylbenzoyladenosine (FSBA) and 2-azido-ATP and identified the amino acids 73–83 and 193–209 as ATP-binding sites within the enzyme. The stoichiometry suggested an equimolar ratio of ATP and 5-LO. This led us

to the assumption that both peptides must be nearby in the tertiary structure forming one ATP binding site. Regarding the crystal structure of Stable-5LOX, this could be only true if 5-LO forms dimers/multimers, as one postulated ATP binding site is located in the C2-like domain, the other in the catalytic domain.

Herein, we describe the first time that human recombinant 5-LO and 5-LO purified from PMNL forms dimers.

Results

Analysis of 5-LO dimer formation by native gel electrophoresis, gel filtration and LILBID-MS

In order to examine the oligomeric state of 5-LO we first performed native gel electrophoresis. Both, recombinant 5-LO that was expressed in *Escherichia coli* as well as 5-LO from PMNL were purified via ATP-agarose and applied to a native Tris-HCl PAGE. The resulting gel was analyzed via Coomassie staining and Western blot. Two major 5-LO bands were identified which suggested that 5-LO may form dimers (Figure 1A).

In order to confirm dimerization of 5-LO, LILBID-MS and gel filtration chromatography was applied. The resulting LILBID spectra of 5-LO WT showed monomeric as well as dimeric and even a little trimeric enzyme (Figure 1B).

For gel filtration, PB/EDTA with addition of 0.15 M up to 1 M NaCl was used. We observed an elution profile consisting of one large peak at an apparent MW of 30 kDa and some smaller peaks which eluted earlier (Figure 1B). The late elution of the 5-LO peak at an apparent MW of 30 kDa is probably due to unspecific interaction with the column material. Repetition of the experiment in PBS/EDTA with addition of 0.5% T20 to reduce this interaction led to the expected MW of 75 kDa for the main peak (Figure 2A) and to a smaller peak at an apparent MW of about 160 kDa. SDS-PAGE and Western blot analysis confirmed that both peaks consist of 5-LO (Figure 2E). Addition of ATP (1 mM) or calcium (1 mM) to the sample buffer and the mobile phase did not change the 5-LO elution profile (data not shown).

In LILBID-MS and in gel filtration, the presence of T20 micelles led to a strong increase in 5-LO dimers indicating that the interaction of 5-LO with micelles induces its dimerization (compare Figures 1B, 2A and 3).

Modification of 5-LO by GSH and diamide

Since 5-LO contains 10 cysteines on the protein surface we wanted to investigate the effect of glutathionylation of the cysteines and the associated changes in 5-LO surface properties on 5-LO dimerization (Figure 4A). Glutathionylation of 5-LO was performed by addition of GSH and diamide as

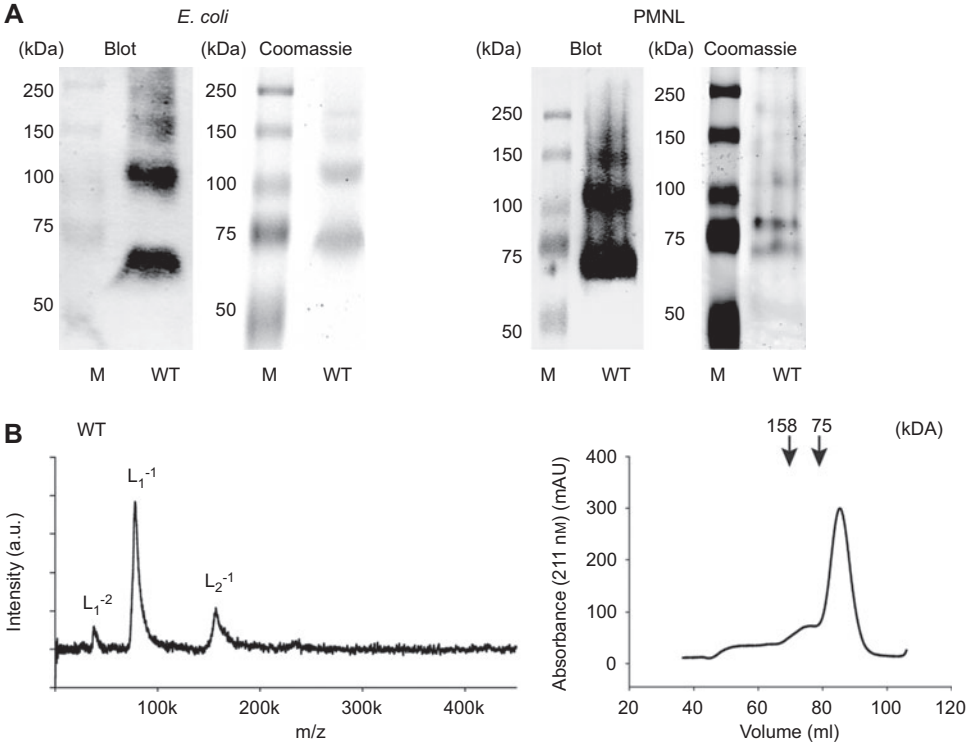

Figure 1 Analysis of 5-LO WT w/o T20.
(A) Native gel electrophoresis of recombinant 5-LO WT and 5-LO from PMNL. 5-LO was detected with anti-5-LO antibody after blotting to a nitrocellulose membrane or with Coomassie blue staining. (B) LILBID spectra of 6.4 μM 5-LO in 100 mM NH_4HCO_3 and gel filtration chromatogram of 2 mg 5-LO in PB/EDTA+0.5 M NaCl.

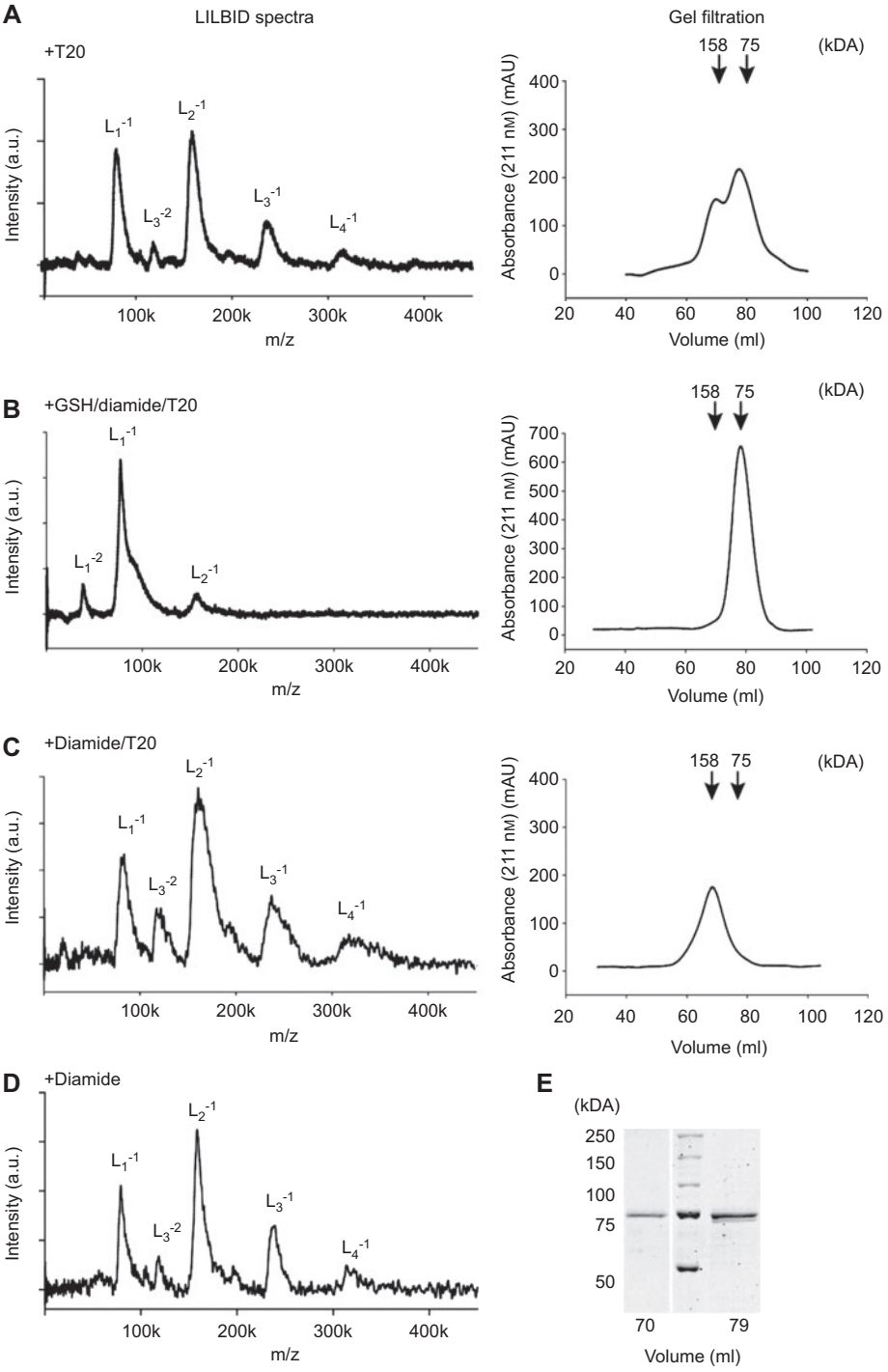

Figure 2 LILBID spectra and gel filtration chromatograms of 5-LO WT in the presence of T20.
Arrows are marking the elution volumes of the reference proteins conalbumin (75 kDa) and aldolase (158 kDa). LILBID spectra of (A) 6.4 μM 5-LO in 100 mM NH_4HCO_3+0.1% T20 and gel filtration of 2 mg 5-LO in PBS/EDTA+0.5% T20, (B) 6.4 μM 5-LO incubated with 25 mM GSH and 2.78 mM diamide for 30 min at 37°C in PBS/EDTA+0.1% T20 followed by buffer exchange to 100 mM NH_4HCO_3+0.1% T20, (C) 6.4 μM 5-LO incubated with 2.78 mM diamide for 10 min at 37°C in PBS/EDTA, afterwards the buffer was exchanged to 100 mM NH_4HCO_3+0.1% T20. The right panels shows the corresponding gel filtrations (mobile phase PBS/EDTA+0.5% T20) of 2 mg 5-LO incubated under the respective conditions of the LILBID analysis. (D) LILBID spectrum of 6.4 μM 5-LO that was preincubated with 2.78 mM diamide for 10 min at 37°C in PBS/EDTA followed by buffer exchange to 100 mM NH_4HCO_3. (E) SDS-PAGE analysis with Coomassie blue staining of gel filtration fractions of the 5-LO monomer (79 ml) and dimer (70 ml) peak from panel A.

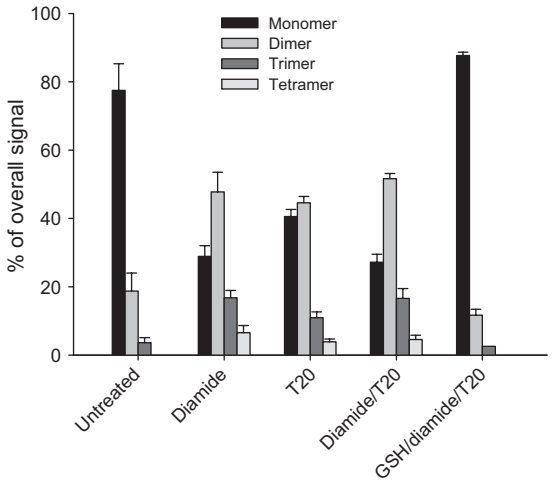

Figure 3 Oligomer distribution of 5-LO WT under different conditions in LILBID-MS analysis. Distribution is shown as percentage of overall signal+SEM (n=3).

oxidizing agent (Kosower and Kosower, 1995). To investigate the influence of a glutathione modification on the oligomeric state of the enzyme, 5-LO was incubated with GSH (10 mM) plus diamide (1 mM) for 30 min at 37°C or diamide alone (1 mM) for 10 min at 37°C.

Treatment of 5-LO with GSH and diamide led to the almost exclusive formation of monomers in LILBID-MS and on gel filtration in the presence of T20 (Figure 2B). LILBID measurements were performed in the presence of T20 (Figure 2A–C), no T20 was added in Figure 2D.

Obviously, treatment of 5-LO with GSH and diamide prevents dimerization. To demonstrate glutathionylation of 5-LO under these conditions, the enzyme was incubated with (^{35}S)-GSH in the presence of diamide. After separation by SDS-PAGE, glutathionylation was detected with a phosphorimager. Maximal glutathionylation of 5-LO was achieved when GSH was combined with diamide and H_2O_2 as oxidant to quench the DTT contained in the (^{35}S)-GSH solution whereas addition of GSH and diamide still leads to lower, but detectable glutathionylation (Figure 5, lanes 3 and 4). To quantify the glutathionylation of 5-LO, free cysteine residues were quantified using Ellman's reagent and HPLC analysis (Chen et al., 2008). We found that treatment of 5-LO with GSH (10 mM) and diamide (1 mM) leads to a reduction in the number of free cysteine residues from 10 in the unmodified 5-LO to nine indicating that one cysteine residue becomes glutathionylated.

Interestingly, treatment of 5-LO with diamide alone for 10 min at 37°C (Figure 2C) completely prevented monomer formation on gel filtration and led to a peak that corresponded to dimers. Elongation of the incubation time led to the formation of even higher molecular complexes. The formation of disulfide bonded 5-LO dimers and oligomers as consequence of the incubation with diamide can be seen in the LILBID spectra both in the presence or absence of T20 (Figure 2C and D). Thus, oxidation of the enzyme and formation of intermolecular disulfide bridges by diamide induced a shift of the size distribution to higher masses concomitant with a depletion of the monomer. For summary of oligomer distribution in LILBID-MS of 5-LO WT see Figure 3.

Analysis of dimer formation in PMNL S100 by gel filtration

PMNL S100 was analyzed by gel filtration in PBS/EDTA. 5-LO activity as well as 5-LO protein (by Western blot) was found in a broad range of fractions from about 60 to 90 ml

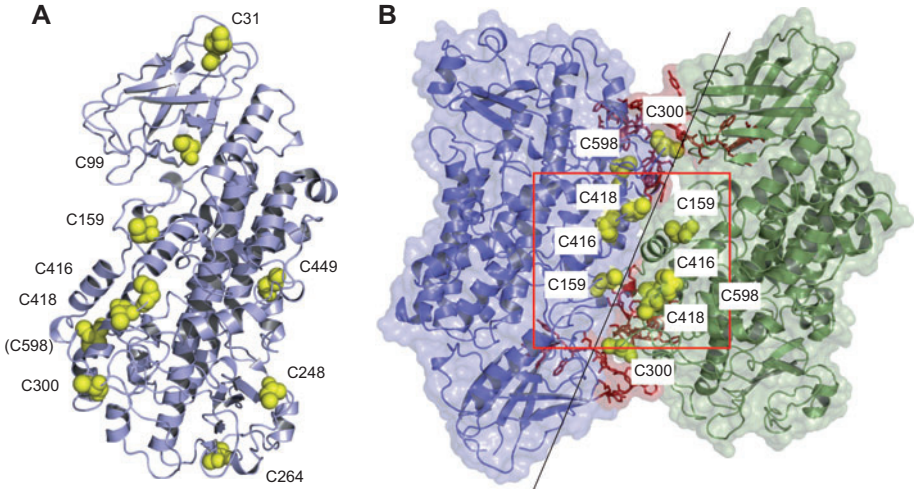

Figure 4 Protein-protein docking of 5-LO and cysteine residues in the putative dimer-interface and on the surface.
(A) Structure of human 5-LO with the surface exposed cysteines (yellow spheres). C598 is partially buried. (B) The most reasonable docking solution, exhibiting a head-to-tail orientation, in cartoon representation with semi-transparent surface. Highlighted are the two proposed ATP binding sites in red, together with the cysteines (yellow spheres) in the predicted dimer interaction interface. The cysteines in the red square (C159, C416, C418) might be sufficiently close to allow for disulfide bond formation.

Figure 5 SDS-PAGE analysis of (^{35}S)-GSH incorporation into 5-LO.

Purified 5-LO WT was incubated with (^{35}S)-GSH and then subjected to SDS-PAGE analysis. GSH incorporation was detected by a Phosphorimager. Lane 1, 5-LO treated with 0.87 mM diamide, 2.5 μCi (^{35}S)-GSH; lane 2, 0.87 mM diamide, 0.87 mM H_2O_2, 2.5 μCi (^{35}S)-GSH; lane 3, 3.48 mM diamide, 2.5 μCi (^{35}S)-GSH; lane 4, 3.48 mM diamide, 0.87 mM H_2O_2, 2.5 μCi (^{35}S)-GSH; lane 5, 0.87 mM diamide; in all lanes: 8.7 mM GSH, 17.4 μl 5-LO.

with the main activity eluting at 75 ml (Figure 6). Since the gel filtration was performed without T20 in the elution buffer, it can be assumed that there is a shift to a smaller MW due to interaction with the column material, comparable to the recombinant 5-LO in the same buffer (dotted line). Despite this, 5-LO activity was also found in fractions that elute at an apparent MW of the dimer indicating that at least a part of the 5-LO could exist as dimer in PMNL.

Molecular modeling and docking of 5-LO

To establish a model of a 5-LO dimer, we used the crystal structure of engineered human 5-LO {Protein Data Bank [PDB, http://pdb.org, (Berman et al., 2000)], ID: 3o8y (Gilbert et al., 2011)}. Gilbert et al. mutated or deleted several amino acids to obtain the so-called 'Stable-5LOX' (Gilbert et al., 2011) thereby enabling crystallization and structure determination. To restore the WT enzyme, we performed *in silico* mutagenesis

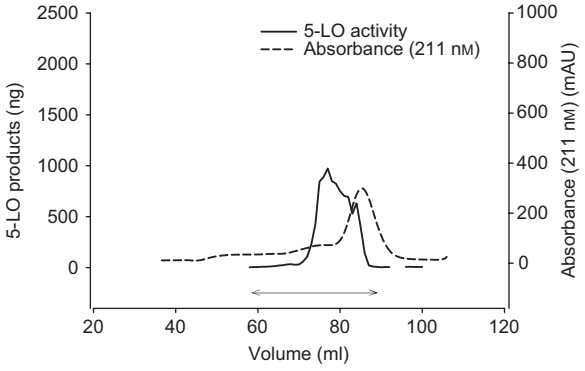

Figure 6 Gel filtration analysis of recombinant 5-LO and PMNL S100.

Gel filtration chromatography of 2 mg purified 5-LO (dotted line) and of PMNL S100 (continuous line) from 2×10^9 cells using PBS/EDTA as mobile phase. 5-LO in the PMNL S100 was recorded by determination of 5-LO activity in the fractions and detection of 5-LO by Western blot analysis with 5-LO antibody (marked with arrow; elution volume 60–90 ml).

and constructed the completed structure of 5-LO WT. For this structure, we predicted potential dimerization sites using four independent software tools. All proposed interfaces (Figure 7) have one side of 5-LO in common, which is flanked by the two putative ATP binding sites K73-K83 and F193-K209 (Figure 7A). The predicted interaction site was then used to evaluate the proposed complex conformations by protein-protein docking performed with the protein docking and clustering technique ClusPro. ClusPro was the best performing server in the last round of CAPRI (Critical Assessment of PRediction of Interactions), a community wide experiment on the comparative evaluation of protein-protein docking for structure prediction (http://www.ebi.ac.uk/msd-srv/capri/) (Janin, 2005). Suggested docked conformations were filtered so that only those complexes were retained whose dimerization site was in agreement with the predicted interface region. Assuming that both proposed ATP binding regions form a coherent ATP binding site, which is possible in a putative 5-LO dimer/multimer, we considered only those complexes fulfilling these criteria. Among these complexes, we selected the number one ranked docking solution as final model (Figure 4B). It exhibits coherent ATP binding sites, matches the predicted interface regions, and represents the biggest cluster of docking solutions; therefore it was ranked highest by the clustering algorithm. This final model constitutes the 5-LO subunits in a head-to-tail orientation, where the C2-like domain of one subunit interacts with the catalytic domain of the other. We found four cysteines in the putative interface three of which (C159, C416, C418) might be sufficiently close to allow for intermolecular disulfide bond formation (Figure 4B), which might explain the observed diamide-induced dimerization.

The reactivity of protein thiols depends on the pK_a value and the accessibility of the thiol, both of which can vary widely. Although protein thiols typically have pK_a values of 8.5–9, these can largely vary depending on the local environment of the cysteine residue (Gilbert, 1984; Simplicio et al., 1998). Therefore, we calculated the pK_a values for the cysteines of 5-LO using the PROPKA program (Li et al., 2005; Bas et al., 2008). All of the predicted interface cysteines have calculated pK_a values of around 9 in the protein environment (C159: 8.5; C300: 9; C416: 8.5; C418: 9; C598: 9.3) which is in agreement with possible glutathionylation/disulfide-bond formation.

Evaluation of the predicted dimer interface

We compared the predicted 5-LO interface with interfaces of 534 non-homologous homodimers. Therefore we used the PROTORP server (Reynolds et al., 2009), which analyzes protein-protein complex formation by calculating a series of physical and chemical parameters of the protein interaction sites that contribute to the binding free energy of the association. These parameters include size and shape, intermolecular bonding, residue and atom composition, as well as secondary structure contributions. The protein association parameters for our dimer model were calculated and compared to those observed in known homodimers (Figure 8A; for abbreviations see supplementary Table S1). For 24 out of the 26 computed parameters the values for the predicted 5-LO dimer are

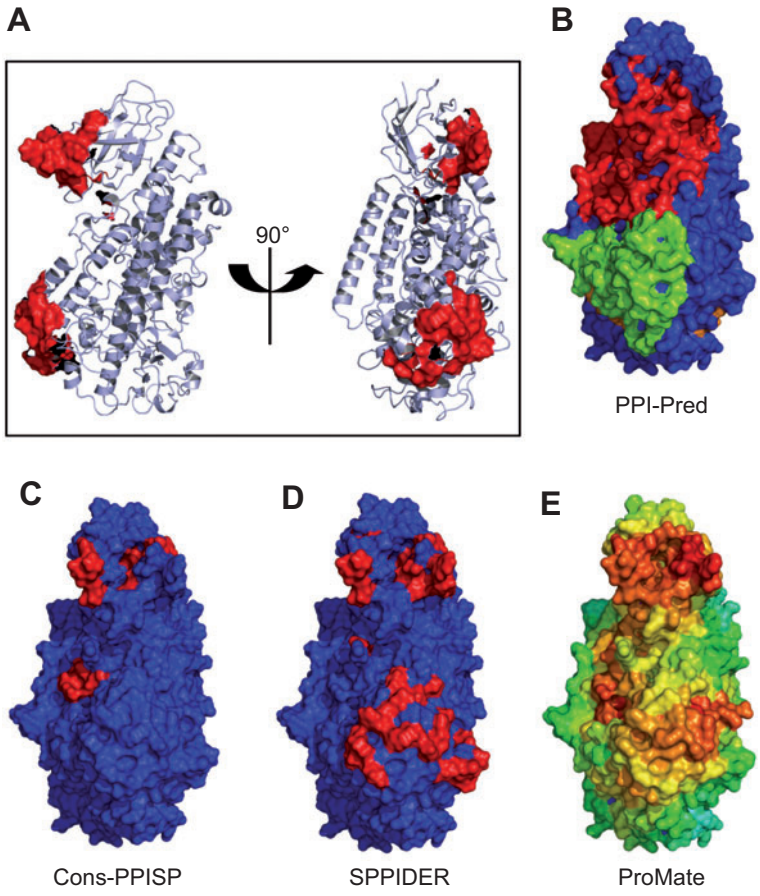

Figure 7 Prediction of protein-protein interaction sites of 5-LO.
(A) Cartoon representation of the tertiary structure of 5-LO. Postulated ATP binding sites are shown as red surface. The orientation of the right hand figure was kept for figures B-E, with the surface colored according to the predicted probability of a protein-protein interaction interface (red: highest probability, green: lower and blue: lowest probability): (B) PPI-Pred, (C) cons-PPISP, (D) SPPIDER, and (E) ProMate prediction.

within the mean±SD of the known complexes. Deviations from a 'typical' homodimer were detected for the total number of surface residues (858.0 instead of 380.5±202.6) and the expected percentage of β-sheets in the interface (20.2±19.4) as no β-sheets are predicted for 5-LO.

Mutation of four cysteines prevents diamide-induced 5-LO dimerization

5-LO contains 13 cysteines and according to the restored 5-LO WT 10 of the cysteines are located on the protein surface. Four of these cysteines are located close to each other at a putative reactive site, which could be important for the dimer formation in a head-to-tail conformation (*cf*. Figure 4). In order to test the hypothesis that this interface is involved in 5-LO dimer formation and that these four cysteines are involved in diamide-induced 5-LO dimerization by formation of intermolecular disulfide bridges, we designed a 4C mutant in which four cysteines (C159S, C300S, C416S, C418S) were replaced with serines. The resulting gel filtration chromatogram of the 4C mutant in presence of T20 and after preincubation with GSH and diamide was similar to the chromatogram of the unmodified and modified WT (Figures 2A, B, and 9A, B). When the 4C mutant was treated with diamide only, the majority of the 4C 5-LO still eluted as monomer and only a minor fraction eluted as dimer (Figure 9C) whereas no monomer was detectable with the WT 5-LO under these conditions (Figure 2C). Formation of covalent dimers by diamide was analyzed with SDS-PAGE without addition of β-mercaptoethanol and detected by Coomassie staining. As shown in Figure 10, diamide-treated WT 5-LO gives a main band at an apparent molecular weight of about 150 kDa, whereas the main band of the 4C mutant was detected at 75 kDa. After boiling of the protein samples with β-mercaptoethanol, only one band was detectable with SDS-PAGE at 75 kDa with WT 5-LO as well as with the 4C mutant indicating that the dimers a linked via disulfide bridges. Similarly, in PMNL only 5-LO monomers were observed when 5-LO was analyzed under denaturing conditions both in the presence and absence or presence of β-mercaptoethanol (Figure 10) indicating that the 5-LO dimers observed under non-denaturing conditions (Figure 1A) are not covalently linked.

In LILBID-MS, the 4C mutant existed almost exclusively as monomer, even in presence of T20 or diamide suggesting that the four cysteines exchanged to serines in the 4C mutant

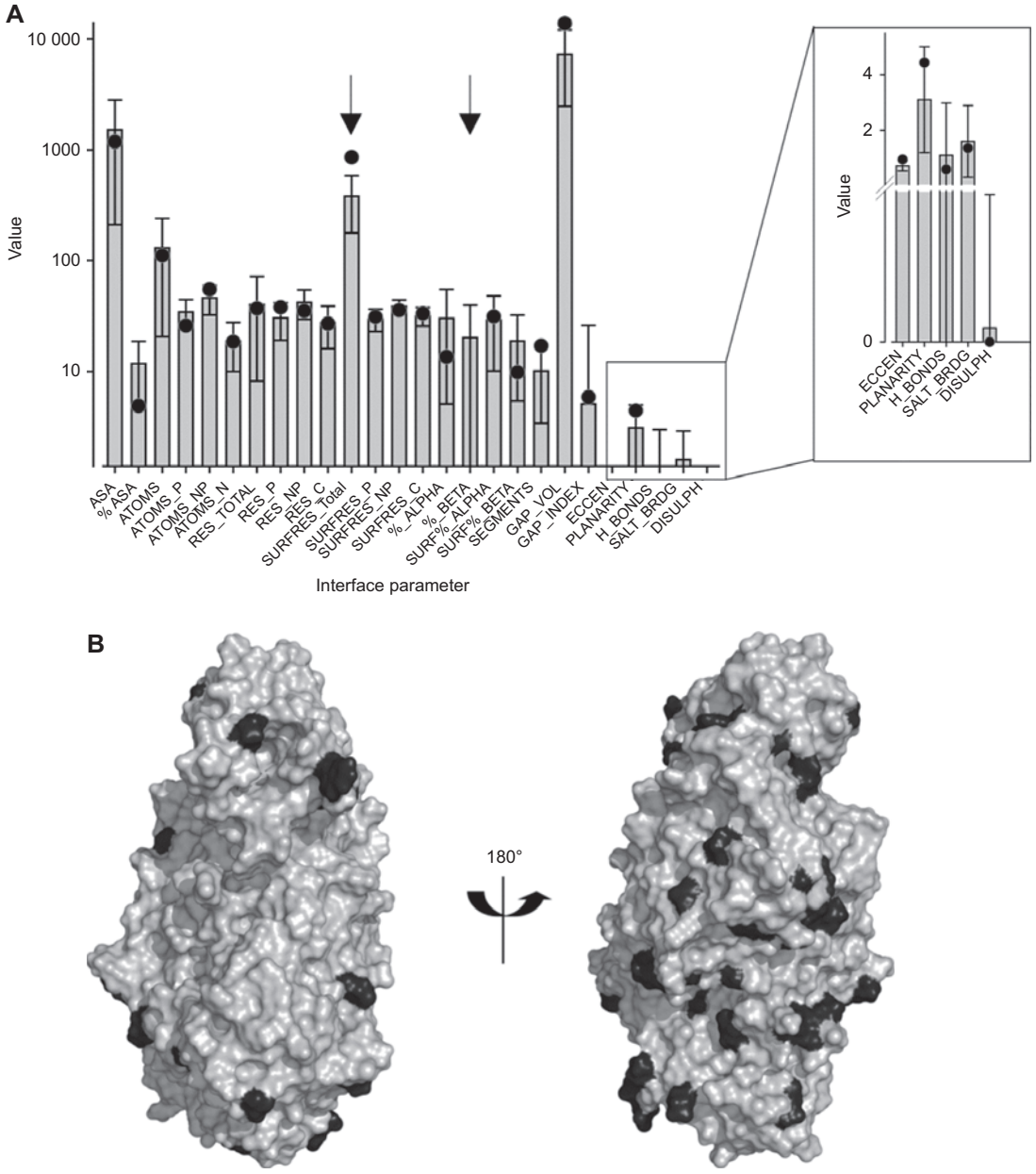

Figure 8 Evaluation of the 5-LO protein-protein dimer interface.

(A) Interface parameters for the protein-protein interaction interface of the 5-LO dimer (black dots) were calculated using PROTORP and compared to the pre-calculated interface parameter distribution of the PROTORP homodimer dataset (grey bars). Data shown are mean values ± SD. Arrows indicate out-of-range values for 5-LO. Hydrogen-bond, salt bridge and disulfide bond values were normalized to 100 Å^2 interface area. For abbreviations, see Table S1. (B) Surface representation of the predicted 5-LO dimer interface, which is conserved between rat and human 5-LO. The left panel presents the interface in the same orientation as in Figure 7, on the right panel the structure is rotated by approximately 180°. The conserved surface is represented in gray, the amino acids that are not conserved are highlighted in black.

are mainly responsible for diamide-induced dimerization of the 5-LO WT enzyme (Figure 9).

Functional studies on 5-LO WT and 4C mutant

5-LO WT and the 4C mutant show similar catalytic activities indicating that the mutations do not significantly alter the 5-LO structure (Table 1). When 5-LO was incubated in the presence of T20, the specific activity was reduced from 534 to 86 ng/μg protein (Table 1) so that it retained only about 15% of its normal activity and activity loss increased with time leading to almost no detectable products when 5-LO was kept in a T20 containing buffer overnight before the activity was determined. This activity loss explains the low specific activity of the enzyme after gel filtration overnight in the presence of T20 (about 4 ng 5-LO products per μg protein). When

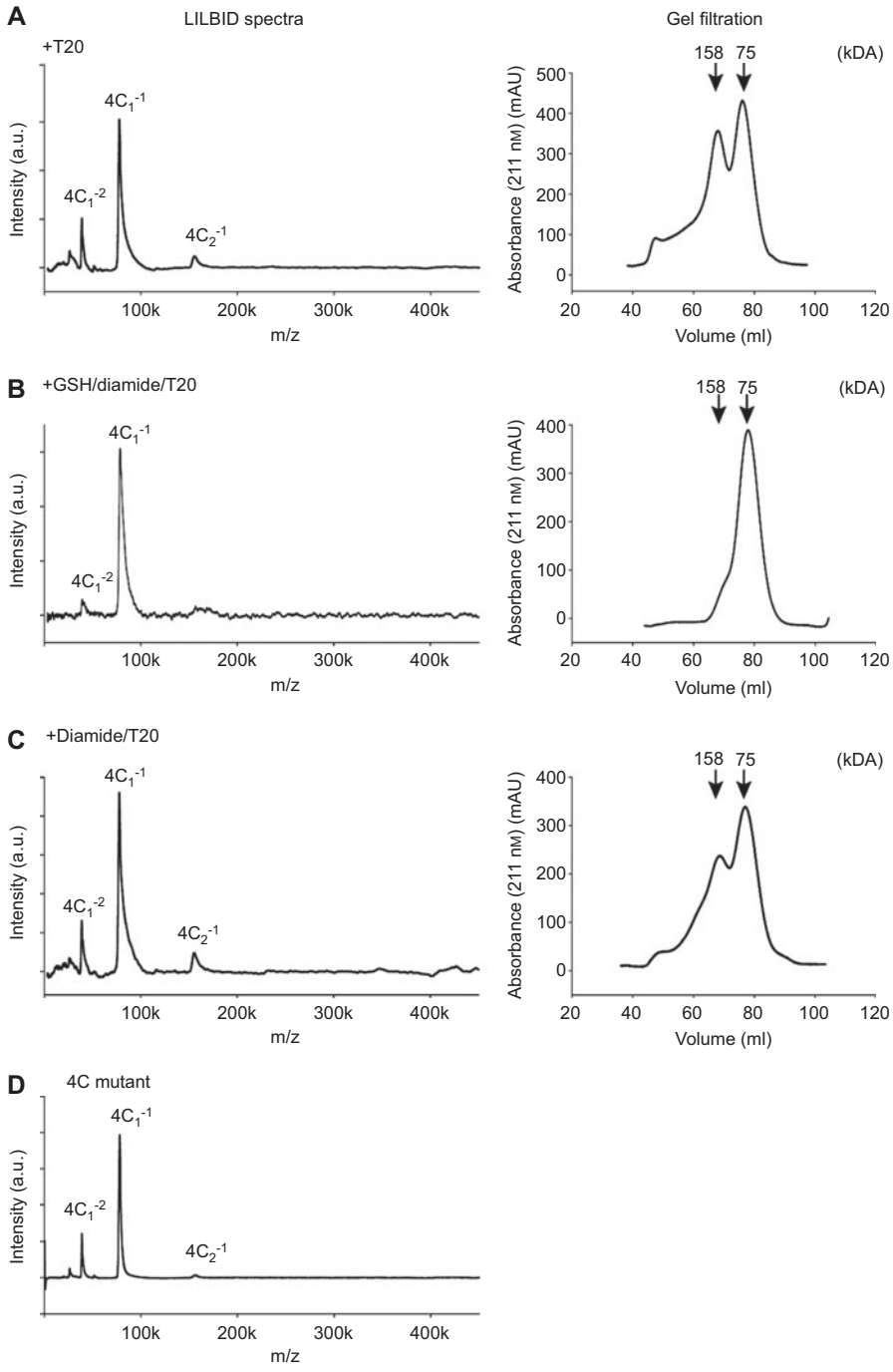

Figure 9 LILBID spectra and gel filtration chromatograms of 4C mutant.
Arrows are marking the elution volumes of the reference proteins conalbumin (75 kDa) and aldolase (158 kDa). LILBID spectra of (A) 6 µM 4C in 100 mM NH_4HCO_3+0.1% T20, (B) 6 µM 4C mutant incubated with 25 mM GSH and 2.78 mM diamide for 30 min at 37°C in PBS/EDTA+0.1% T20, afterwards the buffer was exchanged to 100 mM NH_4HCO_3+0.1% T20, (C) 6 µM 4C mutant incubated with 2.78 mM diamide for 10 min at 37°C in PBS/EDTA, afterwards the buffer was exchanged to 100 mM NH_4HCO_3+0.1% T20 and (D) 6 µM 4C mutant in 100 mM NH_4HCO_3. The right panels show the gel filtration analysis (mobile phase PBS/EDTA+0.5% T20) of 2 mg 4C mutant after incubation under the same conditions as for LILBID analysis.

freshly purified 5-LO was treated with diamide for 10 min, 5-LO activity was reduced from 534 to 23 ng/µg protein which corresponds to about 4% of the activity of the control (Table 1). In contrast, diamide did not inhibit the 4C mutant which is of interest since the reagent also failed to induce dimerization of the 4C mutant (Figure 9). Also, the inhibitory effect of T20 was less pronounced with the 4C mutant. Combined GSH and diamide treatment led to similar activities as in the

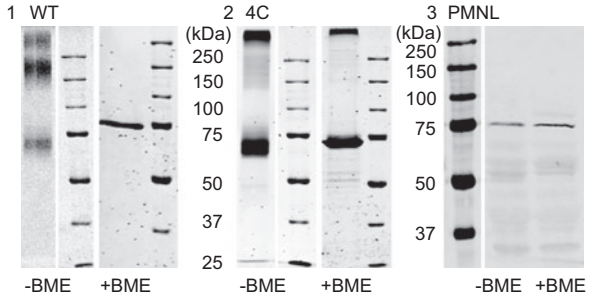

Figure 10 SDS-PAGE analysis of WT 5-LO, 4C mutant and PMNL S100.
Coomassie staining with or without BME of either (1) WT 5-LO or (2) 4C mutant treated with 1 mM diamide and (3) WB of PMNL S100 with or without BME.

Table 1 Enzyme activity of 5-LO WT and the 4C mutant.

	WT 5-LO (ng products/μg protein)	4C 5-LO (ng products/μg protein)
w/o	534±7	436±11
GSH/diamide	557±5	442±8
Diamide	23±1	486±19
T20	86±3	299±19
T20/GSH/ Diamide	72±4	258±3
T20/diamide	9±2	299±5

Purified protein was either used without or with preincubation with 10 mM GSH and 1 mM diamide for 30 min at 37°C or with 1 mM diamide for 10 min at 37°C. Activity assays were performed in PBS/EDTA with 2 mM Ca^{2+}, 1 mM ATP and 20 μM AA with or without 0.5% T20. Enzyme activity is given as ng products per μg protein ± SEM (n=3).

untreated control in the WT enzyme as well as the 4C mutant, suggesting that glutathionylation does not significantly affect 5-LO activity (Table 1).

Discussion

In this work we investigated the dimerization of human 5-LO. The protein plays a key role in leukotriene formation in inflammation and host defense reactions (Samuelsson, 1983). Although it was never studied in detail, 5-LO is generally considered to be a monomeric enzyme. It catalyzes two different reaction steps, consisting of an initial oxygenation step at C5 of arachidonic acid, followed by dehydration and formation of leukotriene A_4. This led us to speculate that 5-LO could form a dimeric complex, where one monomer of the homodimer catalyzes the generation of 5-HPETE which is then transferred to the other monomer for the formation of LTA_4. Alternatively, for COX which catalyzes the initial steps in prostaglandin biosynthesis by the oxygenation of arachidonic acid, Yuan et al. (2009) showed that COX forms dimers, where one substrate molecule binds with high affinity to one COX site and facilitates the oxygenation of arachidonic acid by the other catalytic partner (Yuan et al., 2009). According to these data we assumed that one monomer of the 5-LO could be the catalytically active partner whereas the other monomer has a regulatory function, e.g., *via* its pseudoperoxidase activity (Riendeau et al., 1991).

By gel filtration, native PAGE and LILBID-MS analysis, we found that 5-LO can form dimers and that dimer formation is enhanced in the presence of T20 micelles. Rechromatography of the monomeric peak leads again to the typical monomer/dimer pattern indicating that there is a dynamic balance between monomers and homodimers (data not shown). Neither calcium nor ATP enhanced 5-LO dimerization. 5-LO dimers were reported for rat 5-LO in the presence of calcium, and 5-LO activity was attributed to the dimeric form (Parker and Aykent, 1982). With the human enzyme, we cannot confirm this observation. In accordance with Hammarberg et al. (Hammarberg and Rådmark, 1999) we found no evidence that Ca^{2+} promotes 5-LO dimer formation. This is supported by our diamide experiments. Treatment of 5-LO with GSH/diamide leads to glutathionylation of 5-LO which alters the surface properties of 5-LO and prevents dimer formation as shown with LILBID-MS and gel filtration. However these 'forced' 5-LO monomers displayed similar catalytic activity as the untreated enzyme suggesting that monomers seem to have similar catalytic properties as the untreated enzyme consisting of monomers and dimers (Table 1).

Though, different reaction kinetics for both quaternary structures are conceivable, similarly to what was already discussed for 12-LO (Aleem et al., 2008) and 15-LO2 (Wecksler et al., 2009). An impact of dimerization on the reaction kinetics is presumable due to the observation that the predicted dimer interface is located at the proposed substrate and oxygen entry site of LOs (Ivanov et al., 2010). Although an entry channel to the active site is not directly present in the crystal structure of 5-LO, substrate entry to the catalytic site is expected via conformational changes by amino acids of the so called 'FY-cork' in this region that closes the active site (Gilbert et al., 2011). However, due to the dynamics of the monomer/dimer equilibrium and the very low enzymatic activity of the covalently linked dimers generated by diamide treatment, kinetic experiments on monomers or dimers are difficult to perform. At present, we cannot rule out that dimerization leads to a shift in the 5-LO product pattern.

Addition of diamide to 5-LO (without GSH) yielded mainly dimers and to a low extent even trimers or tetramers depending on the incubation time as shown by gel filtration and LILBID-MS. These 5-LO dimers were also detected by SDS-PAGE (in the absence of β-mercaptoethanol) whereas the SDS-PAGE bands corresponded to the 5-LO monomer when β-mercaptoethanol was added indicating that diamide induces 5-LO dimers in which both proteins are linked by intermolecular disulfide bridges. Interestingly, the covalently linked 5-LO dimers displayed a rather low catalytic activity. This could be explained by intermolecular disulfide bonds that are formed between both monomers and thus according to our

model block the entrance to the catalytic center or avoid a conformational change that is necessary for catalytic activity.

For establishing a model of the 5-LO/5-LO interaction, we used the just-deposited crystal structure of human 5-LO [PDB ID: 3o8y (Gilbert et al., 2011)] and restored the WT enzyme (*in silico* mutation and insertions of the modified amino acids). 3o8y shows a crystallographic dimer, which is not a thermodynamically stable complex (Shang et al., 2011). Therefore, this assembly might solely rise from crystal-packing. Again, (i) 3o8y was engineered which might affect its oligomeric state and (ii) since our observations suggest a monomer-dimer equilibrium the conformation of the weak dimer might not be captured in the crystal structure where the crystallization conditions can lead to numerous non-physiological associations (Dafforn, 2007). By using computational prediction algorithms for protein-protein interaction sites, we established a model for a 5-LO dimer (Figure 4B). Protein-protein interfaces are evolutionarily more conserved than the rest of the protein surface, which has recently been verified using a large protein structural dataset (Choi et al., 2009). This might also be true for weak dimers that are in equilibrium with the monomer in solution (Dey et al., 2010). Thus, we analyzed the conservation of the predicted dimer interface of human 5-LO (Figure 8B). The results suggest that the predicted interface is, apart from the C2-like domain region and in contrast to the rest of the surface, conserved between rat and human 5-LO. Predicted interface parameters support the feasibility of the 5-LO dimer. In our model, four cysteines are located in the interface domain, three of which (C159, C416, C418) are in close spatial proximity suggesting disulfide bridge formation upon diamide treatment. In order to verify our dimer model, we mutated all four cysteine residues and found that mutation of these cysteines largely prevent diamide-induced dimer and oligomer-formation. This is in line with the observation that diamide treatment of the 4C mutant does not inhibit its catalytic activity whereas the WT-enzyme is strongly inhibited. Furthermore, since we have demonstrated that the 4C mutant exists mostly as a monomer in the presence of GSH and diamide, one could speculate that GSH binds to C598, which is located in the suggested dimer interface (*cf.* Figure 4), thereby preventing dimerization of 5-LO. Another argument supporting our dimer model and the head-to-tail orientation of the dimer is the location of the ATP binding site, where two otherwise distant tryptophans, which were previously labeled by azido-ATP (Zhang et al., 2000), are in close proximity to each other (Figure 4B). Such a model, where two ATP molecules are bound by the dimer, is in agreement with the previously reported equimolar ratio of 5-LO and ATP (Zhang et al., 2000). Although the experimental results correlate well with the proposed dimer model, we are fully aware that molecular modelling is prone to errors. Nevertheless, as this is the first suggested model of the putative dimer of 5-lipoxygenase, we hope that it will serve as a valid working tool for generating hypotheses. The herein described 5-LO dimerization interface opens up novel opportunities for the design of inhibitors. The feasibility of this approach, designing protein-protein interaction inhibitors, has been demonstrated recently (for review see González-Ruiz and Gohlke, 2006; Grosdidier et al., 2009). Up to now, there are three main types of direct 5-LO inhibitors known: iron ligand type, redox type, and non-redox type inhibitors. (Ford-Hutchinson et al., 1994). Due to several short comings, only one 5-LO inhibitor could reach the market to date, the iron ligand type inhibitor zileuton (Carter et al., 1991). The interference with 5-LO function via modulation of the protein-protein complex might open up a novel approach to identify small molecule inhibitors to interfere with LT-mediated diseases. It should also be mentioned that the proposed model represents a dimeric complex only and that higher oligomers might exhibit different conformations.

Interestingly, our LILBID-MS-data suggest that T20 micelles promote 5-LO dimerization (Figure 3). Assuming that T20 micelles mimic cell membranes and thus provide a lipophilic surface for 5-LO to interact with, it is possible that in stimulated intact cells, interaction of 5-LO with the membrane after translocation from the cytosol induces dimerization. Arachidonic acid, either supplied exogenously or released by $cPLA_2$ has been shown to induce 5-LO translocation which could be blocked by a FLAP inhibitor (Flamand et al., 2006). 5-LO dimerization after 5-LO translocation and interaction with FLAP is supported by a previous observation where an 186 kDa 5-LO containing complex was found in cross-linking experiments in Sf9 cells when FLAP was coexpressed but not in the absence of FLAP (Plante et al., 2006). Since FLAP is a membrane-bound protein which is required for AA transfer after 5-LO translocation to the nuclear membrane following cell stimulation it might be possible that interaction of 5-LO with the membrane and FLAP triggers dimerization and leukotriene formation.

An interesting phenomenon is the increased dimerization of the WT enzyme by T20 as shown by LILBID analysis (Figure 2A) which is accompanied with a 85% decrease in 5-LO activity whereas the 4C mutant is only inhibited by 30% and does not show dimerization after short-term exposure to T20 in LILBID analysis (Figure 9D). This might give a hint that 5-LO dimers show reduced catalytic activity but it might on the other hand simply be due to the fact that the 4C mutant is more resistant to detergent treatment.

From our data it is clear that the 5-LO monomer shows full catalytic activity. Furthermore, our data show for the first time that leukotriene biosynthesis obviously does not require 5-LO dimerization. However, our study gives only limited hints on the catalytic activity of the dimer. The low enzyme activity observed after diamide-induced dimerization and in the presence of T20 micelles could be related to the covalent linkage of the dimers and to detergent effects, respectively. The fact that T20 also inhibits enzyme activity of the monomeric GSH/diamide-treated 5-LO suggests that the inhibition of 5-LO activity is not related to dimerization. In the native enzyme, it is impossible to selectively detect the activity of the dimer as gel filtration experiments with rechromatography of the monomeric peak led to the usual monomer/dimer distribution again.

Taken together, we could show that 5-LO can form dimers and that there is a dynamic equilibrium between the monomeric and dimeric form. Treatment of 5-LO with GSH and diamide prevents dimerization whereas addition of diamide alone leads to disulfide-linked 5-LO dimers and oligomers. The 5-LO monomer displayed similar catalytic properties as the native enzyme suggesting that dimerization is not required for leukotriene biosynthesis.

However, due to the nuclear localization of 5-LO and its association with euchromatin or to its interaction with dicer, other biological roles were proposed for 5-LO apart from leukotriene biosynthesis, such as regulation of gene expression or miRNA processing, respectively (Woods et al., 1995; Dincbas-Renqvist et al., 2009). Thus, dimerization could be of relevance for the proposed alternative 5-LO functions. In our gel filtration experiments with PMNL supernatants, 5-LO eluted in fractions corresponding to the monomer but the enzyme was also detected in fractions corresponding to the dimer and to higher molecular weights. Furthermore, purified 5-LO from PMNL also formed dimers. A possible explanation could be that a part of the 5-LO exists as dimer and/or in a complex with other soluble proteins. It is known that 5-LO in B-lymphocytes can be activated by treatment with diamide (Jakobsson et al., 1992). Thus, it is reasonable to assume that in the presence of high intracellular GSH levels, diamide leads to the glutathionylation of 5-LO. This could, for example, prevent the interaction of 5-LO with an endogenous inhibitor.

Materials and methods

Site-directed mutagenesis

Selected cysteine codons were mutated by using the QuikChange kit from Stratagene according to manufacturer's protocol (for primer sequence see Table 2). Mutations were confirmed with the ABI PRISM dye terminator cycle-sequencing ready-reaction kit (PerkinElmer, Waltham, MA, USA), followed by analysis on a PRISM 377 sequencer (Applied Biosystems, Carlsbad, CA, USA).

Expression and purification of mutated and WT 5-LO

Recombinant 5-LO was expressed in *E.coli* BL21 (DE3) cells. The cells were transformed with pT3-5LO (kindly provided by Olof Rådmark), and preparation of the enzyme was performed as described previously (Fischer et al., 2003). Further purification was performed by anion exchange column chromatography as described previously (Brungs et al., 1995). In brief, the ATP-eluate (10 ml) was loaded on a ResourceQ 6 ml column (GE Healthcare, Uppsala, Sweden). Buffer A was phosphate-buffer 0.05 mM, pH 7.4 containing 1 mM EDTA, buffer B was buffer A plus 0.5 M NaCl. The elution of the 5-LO was performed in a gradient from 0% to 100% buffer B and the enzyme eluted at about 40% buffer B. Either the partially purified 5-LO obtained after ATP-agarose (~90% purity) or purified 5-LO (~98% purity) was used for the experiments.

Isolation of PMNL from leukocyte concentrates

Blood bags were combined and diluted 1:1 (v:v) with PBS pH 7.4. To each 40 ml of diluted concentrates, 10 ml of dextrane-PBS solution (100 g/l) were added, mixed and sedimented for 30 min. Each 10 ml Nycoprep medium were overlaid with 40 ml of the supernatants and centrifuged at 800 *g* for 10 min at room temperature without deceleration. The supernatant was discarded and the pellet was resuspended in 50 ml ice-cold PBS pH 7.4. After re-centrifugation at 300 *g* for 10 min at room temperature with deceleration, the supernatant was discarded and the pellets were resuspended in 10 ml ice-cold water for lysis of erythrocytes. After 45 s, lysis was stopped by adding 40 ml PBS pH 7.4 at room temperature. The cells were centrifuged at 200 *g* for 10 min, washed with PBS pH 7.4 and lysed again. After re-centrifugation at 200 *g* for 10 min at room temperature, the pellet was resuspended in glucose/PBS medium (1 mg/ml).

Sample preparation and gel filtration of recombinant 5-LO

Modified 5-LO was obtained by incubating 2 mg of 5-LO with GSH (10 mM), GSSG (5 mM) or GSH (10 mM) plus diamide (1 mM) for 30 min at 37°C or by incubation with diamide alone (1 mM) for 10 min at 37°C. 5-LO was applied onto a 16/60 Superdex 200 pg column (GE Healthcare, Uppsala, Sweden) which was eluted with PBS containing 1 mM EDTA with or without addition of 0.5% T20 at a flow rate of 1 ml/min. UV absorbance was recorded at 211 nm. To calibrate the column, the standard proteins conalbumin (75 kDa), aldolase (158 kDa) and ferritin (440 kDa monomer, 880 kDa dimer) were used for each buffer.

Sample preparation and gel filtration of PMNL S100

A total of 2×10^9 cells were resuspended in PBS/EDTA containing 60 µg/ml soybean trypsin inhibitor, 0.4 mM PMSF and 10 µg/ml leupeptin, homogenized by sonication (6×10 s) and centrifuged at 100 000 *g* for 70 min at 4°C. Afterwards, the resulting supernatant was applied to the gel filtration column and eluted with PBS/EDTA at a flow rate of 1 ml/min.

Radioactive glutathione binding assay

5-LO (2.5 µM) was incubated with GSH (8.7 mM), (^{35}S)-GSH (2.5 µCi) and diamide (0.87 mM) for 30 min at 37°C and then analyzed via SDS-PAGE. (^{35}S)-GSH labeled proteins were detected using a Phosphorimager (Fuji FLA-3000, Fujifilm, Düsseldorf, Germany).

Table 2 List and sequence of oligonucleotide primers used for construction of the 4C mutant.

Primer	Sequence (5′→3′)	
	Forward	Reverse
C159S	CGATGCCAAAAGCCACAAGGATTTACCCCG	CGGGGTAAATCCTTGTGGCTTTTGGCATCG
C300S	CAAAACAGACCCCAGCACACTCCAGTTCCTG	CAGGAACTGGAGTGTGCTGGGGTCTGTTTTG
C416/418S	GCAGCTCATCAGCGAGAGTGGCCTCTTTGAC	GTCAAAGAGGCCACTCTCGCTGATGAGCTGC

Determination of free cysteine residues using Ellman's reagent and HPLC analysis

5-LO purified by ion exchange chromatography was concentrated using Amicon Ultra-4 (10 kDa) columns (Millipore, Billerica, MA, USA), incubated with GSH and diamide as described above and subjected to the determination of thiols via HPLC quantification as described previously (Chen et al., 2008).

Determination of product formation of 5-LO

For determination of the activity of recombinant 5-LO and PMNL S100, 1 mM ATP was added to the resulting fractions of the gel filtration, the samples were prewarmed for 30 s at 37°C and 2 mM $CaCl_2$ and 20 μM AA were added to a final incubation volume of 1 ml. The reaction was stopped after 10 min by the addition of 1 ml ice-cold methanol. The 5-LO products were extracted and analyzed by HPLC using PGB_1 as internal standard as described previously (Werz and Steinhilber, 1996).

SDS-PAGE and Western blot analysis

Samples derived from the gel filtration were mixed with 5×SDS-PAGE loading buffer (250 mM Tris/HCl, pH 6.8, 5 mM EDTA, 50% glycerol, 10% SDS, 0.05% BPB, 10% BME) and heated for 5 min at 95°C. The proteins were separated according to the protocol of Laemmli (Laemmli, 1970). When disulfide bonds were investigated the samples where boiled without addition of BME. The resulting gels were either stained with Coomassie blue or analyzed by Western blot (Michel et al., 2008). The antibodies were diluted in TBS plus 0.05% FCS as follows: mouse 5-LO primary monoclonal antibody 1:1000 (produced in-house, binds to the catalytic domain), anti-mouse alkaline phosphatase-conjugated antibody 1:1000.

Laser induced liquid bead ion desorption (LILBID) measurement

The effect of diamide and glutathione were reassessed by a laser mass spectrometry (MS) method termed LILBID (laser induced liquid bead ion desorption). Details of the LILBID technique have been published elsewhere (Morgner et al., 2006). Briefly, aqueous micro droplets are transferred into vacuum where they are irradiated one by one by pulsed infrared laser radiation, with a wavelength corresponding to the water absorption (λ=3 μm) leading to stretching vibration of the water molecules and transfer of energy to the droplets. Beyond a certain laser intensity threshold, the droplets 'explode' and preformed ions are ejected from the liquid into the gas phase where they are analyzed by time-of-flight mass spectrometry (TOF-MS). For LILBID analysis, the phosphate buffer of the 5-LO protein samples was exchanged for a 100 mM ammonium hydrogencarbonate buffer pH 7.4 by utilizing Zeba Micro Spin Desalting Columns to avoid a high background signal that is caused by sodium ions contained in the phosphate buffer. In LILBID samples containing T20, the detergent (0.1%) was added after the buffer exchange except in diamide/glutathione-treated 5-LO samples, T20 was added before buffer exchange to avoid binding of the 5-LO to the buffer exchange column.

In silico restoration of the structure of WT 5-LO

The crystal structure of engineered human 5-LO {Protein Data Bank [PDB, http://pdb.org, (Berman et al., 2000) ID: 3o8y (Gilbert et al., 2011), chain B]} was subjected to *in silico* mutagenesis to restore the WT enzyme. For enabling crystallization and structure determination, Gilbert et al. mutated or deleted several amino acids to obtain the so-called 'Stable-5LOX' (Gilbert et al., 2011) which contains the following mutations: W13E, F14H, W75G, L76S, C240A, C561A, $K^{653}KK^{655} \rightarrow$ ENL, and ΔP40 to D44GS. To restore the WT enzyme, we performed *in silico* mutagenesis of the modified residues and construction of the missing segment using the software package MOE (version 2010.10; Chemical Computing Group, Montreal, QC, Canada), which uses rotamer libraries, loop prediction (Fechteler et al., 1995), and energy minimization to construct the missing or modified residues. Energy minimization was performed using the all-atom force field AMBER99 (Wang et al., 2000) with root mean square (RMS) gradient of 1.

Prediction of protein-protein interaction sites

Putative protein-protein interaction sites of 5-LO were independently calculated using ProMate 2.0 (http://bioinfo.weizmann.ac.il/promate/) (Neuvirth et al., 2004), Cons-PPISP (http://pipe.scs.fsu.edu/ppisp.html) (Zhou and Shan, 2001; Chen and Zhou, 2005), PPI-Pred (http://bmbpcu36.leeds.ac.uk/ppi_pred/) (Bradford and Westhead, 2005), and SPPIDER (http://sppider.cchmc.org/) (Porollo and Meller, 2007). ProMate predicts the location of protein-protein binding sites in unbound proteins by extracting a set of surface patches for the query protein. Using the distributions of the properties that have been found to distinguish binding from non-binding surfaces, the predictor evaluates the probability of each patch to appear in the interface. Cons-PPISP is a consensus neural network method that was trained on known structures of protein-protein complexes. The input to the neural network includes position-specific sequence profiles and solvent accessibilities of each residue and its spatial neighbors. PPI-Pred calculates properties of the protein surface that allow for a distinction of protein-interfaces from the rest of the surface: hydrophobicity, residue interface propensity, electrostatic potential, solvent accessible surface area, surface topography (shape) and sequence conservation. SPPIDER uses relative solvent accessibility fingerprints to discriminate between interacting and non-interacting sites.

Protein-protein docking

The protein docking and clustering technique ClusPro (Comeau et al., 2004) was used to predict a model of the overall structure of the 5-LO dimer using the 'dimer' mode with balanced coefficients. One thousand low energy models were calculated and provided to the clustering algorithm, which clustered the results according to root mean square distance (RMSD). Clusters were ranked according to cluster size and the ten top ranking clusters were retained. We manually evaluated these docking conformations combining the outcome of the protein-protein interaction site predictions and the experimental results.

Evaluation of the predicted dimer interface

The predicted dimer interface of 5-LO was compared with the interfaces of known homodimers using the PROTORP server (Reynolds et al., 2009), which calculates a set of 26 physicochemical parameters exhibited by each protein interface. The dataset consists of 534 non-homologous homodimers. Values for the calculated parameters are given as mean±SD. Hydrogen-bond, salt bridge and disulfide bond values were normalized to 100 $Å^2$ interface area. The parameter 'bridging water molecule' was omitted.

Calculation of cysteine pK_a values

pK_a values of cysteine residues of the restored 5-LO WT structure were calculated using the PROPKA web interface 2.0 (http://propka.ki.ku.dk/) (Li et al., 2005; Bas et al., 2008).

5-LO protein quantification

The 5-LO protein concentration was determined by SDS-PAGE as described above with bovine serum albumin (BSA) as standard. Quantification analysis was performed using an Odyssey® Imaging System (Licor Biosciences, NE, USA).

Native gel electrophoresis

Native gel electrophoresis was performed as described previously (Betts et al., 1999). In brief, the sample was mixed with 3× sample buffer (0.6 ml 50× running buffer, 3 ml glycerol (87%), 0.05% BPB, and 10 ml purified water) and applied to a native gel that consisted of a stacking gel (7× stacking gel buffer: 0.5 M Tris, pH 6.8) and a resolving gel (4× resolving gel buffer: 1.5 M Tris, pH 8.8). All solutions were equilibrated to 4°C and electrophoresis was performed in a cold room at 4°C in native running buffer (50× running buffer: 248 mM Tris, 1.918 M glycine). Electrophoresis was started at 10 mA (300 V max) and increased up to 15 mA when the loading dye bromphenol blue entered the resolving gel. To investigate calcium dependence either 1 mM calcium or 1 mM EDTA was added to all buffers.

Acknowledgments

The study was supported by the Deutsche Forschungsgemeinschaft (FOR 784), the CEF and ECCPS Excellence Clusters.

References

Aleem, A.M., Jankun, J., Dignam, J.D., Walther, M., Kühn, H., Svergun, D.I., and Skrzypczak-Jankun, E. (2008). Human platelet 12-lipoxygenase, new findings about its activity, membrane binding and low-resolution structure. J. Mol. Biol. *376*, 193–209.

Aleem, A.M., Wells, L., Jankun, J., Walther, M., Kühn, H., Reinartz, J., and Skrzypczak-Jankun, E. (2009). Human platelet 12-lipoxygenase: naturally occurring Q261/R261 variants and N544L mutant show altered activity but unaffected substrate binding and membrane association behavior. Int. J. Mol. Med. *24*, 759–764.

Bas, D.C., Rogers, D.M., and Jensen, J.H. (2008). Very fast prediction and rationalization of pKa values for protein-ligand complexes. Proteins *73*, 765–783.

Berman, H.M., Westbrook, J., Feng, Z., Gilliland, G., Bhat, T.N., Weissig, H., Shindyalov, I.N., and Bourne, P.E. (2000). The Protein Data Bank. Nucleic Acids Res. *28*, 235–242.

Betts, S., Speed, M., and King, J. (1999). Detection of early aggregation intermediates by native gel electrophoresis and native western blotting. Methods Enzymol. *309*, 333–350.

Bradford, J.R. and Westhead, D.R. (2005). Improved prediction of protein-protein binding sites using a support vector machines approach. Bioinformatics *21*, 1487–1494.

Brungs, M., Rådmark, O., Samuelsson, B., and Steinhilber, D. (1995). Sequential induction of 5-lipoxygenase gene expression and activity in Mono Mac 6 cells by transforming growth factor β and 1,25-dihydroxyvitamin D3. Proc. Natl. Acad. Sci. USA *92*, 107–111.

Carter, G.W., Young, P.R., Albert, D.H., Bouska, J., Dyer, R., Bell, R.L., Summers, J.B., and Brooks, D.W. (1991). 5-lipoxygenase inhibitory activity of zileuton. J. Pharmacol. Exp. Ther. *256*, 929–937.

Chen, H. and Zhou, H.X. (2005). Prediction of interface residues in protein-protein complexes by a consensus neural network method: test against NMR data. Proteins *61*, 21–35.

Chen, W., Zhao, Y., Seefeldt, T., and Guan, X. (2008). Determination of thiols and disulfides via HPLC quantification of 5-thio-2-nitrobenzoic acid. J. Pharm. Biomed. Anal. *48*, 1375–1380.

Chen, X.S. and Funk, C.D. (2001). The N-terminal "beta-barrel" domain of 5-lipoxygenase is essential for nuclear membrane translocation. J. Biol. Chem. *276*, 811–818.

Chen, Y., Hu, Y., Zhang, H., Peng, C., and Li, S. (2009). Loss of the Alox5 gene impairs leukemia stem cells and prevents chronic myeloid leukemia. Nat. Genet. *41*, 783–792.

Choi, Y.S., Yang, J.S., Choi, Y., Ryu, S.H., and Kim, S. (2009). Evolutionary conservation in multiple faces of protein interaction. Proteins *77*, 14–25.

Comeau, S.R., Gatchell, D.W., Vajda, S., and Camacho, C.J. (2004). ClusPro: a fully automated algorithm for protein-protein docking. Nucleic Acids Res. *32*, W96–W99.

Dafforn, T.R. (2007). So how do you know you have a macromolecular complex? Acta Crystallogr. D Biol. Crystallogr. *63*, 17–25.

Dahlén, S.E., Hedqvist, P., Hammarström, S., and Samuelsson, B. (1980). Leukotrienes are potent constrictors of human bronchi. Nature *288*, 484–486.

Dey, S., Pal, A., Chakrabarti, P., and Janin, J. (2010). The subunit interfaces of weakly associated homodimeric proteins. J. Mol. Biol. *398*, 146–160.

Dincbas-Renqvist, V., Pépin, G., Rakonjac, M., Plante, I., Ouellet, D.L., Hermansson, A., Goulet, I., Doucet, J., Samuelsson, B., Rådmark, O., et al. (2009). Human Dicer C-terminus functions as a 5-lipoxygenase binding domain. Biochim. Biophys. Acta *1789*, 99–108.

Fechteler, T., Dengler, U., and Schomburg, D. (1995). Prediction of protein three-dimensional structures in insertion and deletion regions: a procedure for searching data bases of representative protein fragments using geometric scoring criteria. J. Mol. Biol. *253*, 114–131.

Fischer, L., Szellas, D., Rådmark, O., Steinhilber, D., and Werz, O. (2003). Phosphorylation- and stimulus-dependent inhibition of cellular 5-lipoxygenase activity by nonredox-type inhibitors. FASEB J. *17*, 949–951.

Flamand, N., Lefebre, J., Surette, M.E., Picard, S., and Borgeat, P. (2006). Arachidonic acid regulates the translocation of 5-lipoxygenase to the nuclear membranes in human neutrophils. J. Biol. Chem. *281*, 129–136.

Ford-Hutchinson, A.W., Gresser, M., and Young, R.N. (1994). 5-Lipoxygenase. Annu. Rev. Biochem. *63*, 383–417.

Funk, C.D. (2001). Prostaglandins and leukotrienes: advances in eicosanoid biology. Science *294*, 1871–1875.

Gilbert, H.F. (1984). Redox control of enzyme activities by thiol/disulfide exchange. Methods Enzymol. *107*, 330–351.

Gilbert, N.C., Bartlett, S.G., Waight, M.T., Neau, D.B., Boeglin, W.E., Brash, A.R., and Newcomer, M.E. (2011). The structure of human 5-lipoxygenase. Science *331*, 217–219.

González-Ruiz, D. and Gohlke, H. (2006). Targeting protein-protein interactions with small molecules: challenges and perspectives for computational binding epitope detection and ligand finding. Curr. Med. Chem. *13*, 2607–2625.

Grosdidier, S., Totrov, M., and Fernández-Recio, J. (2009). Computer applications for prediction of protein-protein interactions and rational drug design. Adv. Appl. Bioinform. Chem. *2*, 101–123.

Hammarberg, T. and Rådmark, O. (1999). 5-lipoxygenase binds calcium. Biochemistry *38*, 4441–4447.

Hammarberg, T., Provost, P., Persson, B., and Rådmark, O. (2000). The N-terminal domain of 5-lipoxygenase binds calcium and mediates calcium stimulation of enzyme activity. J. Biol. Chem. *275*, 38787–38793.

Hörnig, C., Albert, D., Fischer, L., Hörnig, M., Rådmark, O., Steinhilber, D., and Werz, O. (2005). 1-Oleoyl-2-acetylglycerol stimulates 5-lipoxygenase activity *via* a putative (phospho)lipid binding site within the N-terminal C2-like domain. J. Biol. Chem. *280*, 26913–26921.

Ivanov, I., Heydeck, D., Hofheinz, K., Roffeis, J., O'Donnell, V.B., Kuhn, H., and Walther, M. (2010). Molecular enzymology of lipoxygenases. Arch. Biochem. Biophys. *503*, 161–174.

Jakobsson, P.J., Steinhilber. D., Odlander, B., Rådmark, O., Claesson, H.E., and Samuelsson, B. (1992). Proc. Natl. Acad. Sci. USA *89*, 3521–3525.

Janin, J. (2005). Assessing predictions of protein-protein interaction: the CAPRI experiment. Protein Sci. *14*, 278–283.

Kosower, N.S. and Kosower, E.M. (1995). Diamide: an oxidant probe for thiols. Methods Enzymol. *251*, 123–133.

Kulkarni, S., Das, S., Funk, C.D., Murray, D., and Cho, W. (2002). Molecular basis of the specific subcellular localization of the C2-like domain of 5-lipoxygenase. J. Biol. Chem. *277*, 13167–13174.

Laemmli, U.K. (1970). Cleavage of structural proteins during the assembly of the head of bacteriophage T4. Nature *227*, 680–685.

Li, H., Robertson, A.D., and Jensen, J.H. (2005). Very fast empirical prediction and rationalization of protein pKa values. Proteins *61*, 704–721.

Luo, M., Jones, S.M., Phare, S.M., Coffey, M.J., Peters-Golden, M., and Brock, T.G. (2004). Protein kinase A inhibits leukotriene synthesis by phosphorylation of 5-lipoxygenase on serine 523. J. Biol. Chem. *279*, 41512–41520.

Matsumoto, T., Funk, C.D., Rådmark, O., Höög, J.O., Jörnvall, H., and Samuelsson, B. (1988). Molecular cloning and amino acid sequence of human 5-lipoxygenase. Proc. Natl. Acad. Sci. USA *85*, 26–30.

Michel, A.A.Y., Steinhilber, D., and Werz, O. (2008). Development of a method for expression and purification of the regulatory C2-like domain of human 5-lipoxygenase. Protein Expr. Purif. *59*, 110–116.

Morgner, N., Barth, H.D., and Brutschy, B. (2006). A new way to detect noncovalently bonded complexes of biomolecules from liquid micro-droplets by laser mass spectrometry. Austral. J. Chem. *59*, 109–114.

Neuvirth, H., Raz, R., and Schreiber, G. (2004). ProMate: a structure based prediction program to identify the location of protein-protein binding sites. J. Mol. Biol. *338*, 181–199.

Parker, C.W. and Aykent, S. (1982). Calcium stimulation of the 5-lipoxygenase from RBL-1 cells. Biochem. Biophys. Res. Commun. *109*, 1011–1016.

Peters-Golden, M. and Brock, T.G. (2003). 5-lipoxygenase and FLAP. Prostaglandins Leukot. Essent. Fatty Acids *69*, 99–109.

Plante, H., Picard, S., Mancini, J., and Borgeat, P. (2006). 5-Lipoxygenase-activating protein homodimer in human neutrophils: evidence for a role in leukotriene biosynthesis. Biochem. J. *393 (Pt 1)*, 211–218.

Porollo, A. and Meller, J. (2007). Prediction-based fingerprints of protein-protein interactions. Proteins *66*, 630–645.

Pouliot, M., McDonald, P.P., Krump, E., Mancini, J.A., McColl, S.R., Weech, P.K., and Borgeat, P. (1996). Colocalization of cytosolic phospholipase A2, 5-lipoxygenase, and 5-lipoxygenase-activating protein at the nuclear membrane of A23187-stimulated human neutrophils. Eur. J. Biochem. *238*, 250–258.

Rådmark, O. (2002). Arachidonate 5-lipoxygenase. Prostaglandins Other Lipid Mediat. *68–69*, 211–234.

Rakonjac, M., Fischer, L., Provost, P., Werz, O., Steinhilber, D., Samuelsson, B., and Rådmark, O. (2006). Coactosin-like protein supports 5-lipoxygenase enzyme activity and up-regulates leukotriene A4 production. Proc. Natl. Acad. Sci. USA *103*, 13150–13155.

Reynolds, C., Damerell, D., and Jones, S. (2009). ProtorP: a protein-protein interaction analysis server. Bioinformatics *25*, 413–414.

Riendeau, D., Falgueyret, J.P., Guay, J., Ueda, N., and Yamamoto, S. (1991). Pseudoperoxidase activity of 5-lipoxygenase stimulated by potent benzofuranol and N-hydroxyurea inhibitors of the lipoxygenase reaction. Biochem. J. *274 (Pt 1)*, 287–292.

Rouzer, C.A. and Samuelsson, B. (1985). On the nature of the 5-lipoxygenase reaction in human leukocytes: enzyme purification and requirement for multiple stimulatory factors. Proc. Natl. Acad. Sci. USA *82*, 6040–6044.

Samuelsson, B. (1983). Leukotrienes: mediators of immediate hypersensitivity reactions and inflammation. Science *220*, 568–575.

Shang, W., Ivanov, I., Svergun, D.I., Borbulevych, O.Y., Aleem, A.M., Stehling, S., Jankun, J., Kuhn, H., and Skrzypczak-Jankun, E. (2011). Probing dimerization and structural flexibility of mammalian lipoxygenases by small-angle X-ray scattering. J. Mol. Biol. *409*, 654–668.

Shimizu, T., Izumi, T., Seyama, Y., Tadokoro, K., Rådmark, O., and Samuelsson, B. (1986). Characterization of leukotriene A4 synthase from murine mast cells: evidence for its identity to arachidonate 5-lipoxygenase. Proc. Natl. Acad. Sci. USA *83*, 4175–4179.

Simplicio, P.D., Cacace, M.G., Lusini, L., Giannerini, F., Giustarini, D., and Rossi, R. (1998). Role of protein-SH groups in redox homeostasis – the erythrocyte as a model system. Arch. Biochem. Biophys. *355*, 145–152.

Wang, J., Cieplak, P., and Kollman, P.A. (2000). How well does a restrained electrostatic potential (RESP) model perform in calculating conformational energies of organic and biological molecules? J. Comput. Chem. *21*, 1049–1074.

Wecksler, A.T., Kenyon, V., Garcia, N.K., Deschamps, J.D., van der Donk, W.A., and Holman, T.R. (2009). Kinetic and structural investigations of the allosteric site in human epithelial 15-lipoxygenase-2. Biochemistry *48*, 8721–8730.

Werz, O. (2002). 5-lipoxygenase: cellular biology and molecular pharmacology. Curr. Drug Targets Inflamm. Allergy *1*, 23–44.

Werz, O. and Steinhilber, D. (1996). Selenium-dependent peroxidases suppress 5-lipoxygenase activity in B-lymphocytes and immature myeloid cells. The presence of peroxidase-insensitive 5-lipoxygenase activity in differentiated myeloid cells. Eur. J. Biochem. *242*, 90–97.

Werz, O., Klemm, J., Samuelsson, B., and Rådmark, O. (2000). 5-lipoxygenase is phosphorylated by p38 kinase-dependent MAPKAP kinases. Proc. Natl. Acad. Sci. USA *97*, 5261–5266.

Werz, O., Bürkert, E., Fischer, L., Szellas, D., Dishart, D., Samuelsson, B., Rådmark, O., and Steinhilber, D. (2002). Extracellular signal-regulated kinases phosphorylate 5-lipoxygenase and stimulate

5-lipoxygenase product formation in leukocytes. FASEB J. *16*, 1441–1443.

Woods, J.W., Coffey, M.J., Brock, T.G., Singer, I.I., and Peters-Golden, M. (1995). 5-Lipoxygenase is located in the euchromatin of the nucleus in resting human alveolar macrophages and translocates to the nuclear envelope upon cell activation. J. Clin. Invest. *95*, 2035–2046.

Yuan, C., Sidhu, R.S., Kuklev, D.V., Kado, Y., Wada, M., Song, I., and Smith, W.L. (2009). Cyclooxygenase allosterism, fatty acid-mediated cross-talk between monomers of cyclooxygenase homodimers. J. Biol. Chem. *284*, 10046–10055.

Zhang, Y.Y., Hammarberg, T., Rådmark, O., Samuelsson, B., Ng, C.F., Funk, C.D., and Loscalzo, J. (2000). Analysis of a nucleotide-binding site of 5-lipoxygenase by affinity labelling: binding characteristics and amino acid sequences. Biochem. J. *351*, 697–707.

Zhou, H.X. and Shan, Y. (2001). Prediction of protein interaction sites from sequence profile and residue neighbor list. Proteins *44*, 336–343.

Received August 21, 2011; accepted October 7, 2011